PCCP

ROYAL SOCIETY OF CHEMISTRY

COMMUNICATION

View Article Online
View Journal

Cite this: DOI: 10.1039/d6cp00348f

Received 30th January 2026,
Accepted 27th March 2026

DOI: 10.1039/d6cp00348f

rsc.li/pccp

Quantum-chemical insights into the design of molecule-modified Pt catalysts for the oxygen reduction reaction

Kohei Tada, *[abc] Shoma Kinugawa,[b] Shin-ichi Yamazaki, [a] Yukichika Kitano,[b] Yasutaka Kitagawa, [bc] Masafumi Asahi, [a] Yoshihiro Chida [a] and Tsutomu Ioroi [a]

The present study provides insights into the rational design of molecular modifiers for oxygen reduction reaction (ORR) catalysts, which are of significant societal interest. Specifically, (1) the strength of modifier–Pt interactions and ORR activity have a volcano-shaped correlation, and (2) the strength is explained using the HOMO of the modifier. These are derived from the coordination bond affinity between the organic modifier and Pt.

Polymer electrolyte fuel cell (PEFC) systems using green hydrogen as fuel have been actively researched because they are key devices for realising a hydrogen society.[1–3] Catalysts are required to drive the oxygen reduction reaction at the cathode, and Pt-based catalysts have been used most widely. However, large amounts of Pt are required because of their insufficient activity and durability.

Surface modification using organic molecules such as melamine has recently attracted attention as a promising approach for simultaneously enhancing the ORR activity and durability of Pt-based catalysts.[4–14] The catalytic activity of metal surfaces is well explained by their d-band centres,[15,16] but melamine molecules do not alter the d-band centres of Pt surfaces.[17–19] The intermediate OH species on Pt is over-stabilised *via* interaction with water molecules near the Pt surfaces, thereby inhibiting the oxygen ORR.[20–25] Both theoretical and experimental studies showed that melamine weakens hydrogen bonding in water molecules near the Pt surface and significantly destabilise the OH species.[18,20] Furthermore, melamine is adsorbed more strongly onto high-index surfaces[8,26]; it therefore preferentially protects under-coordinated Pt atoms that promote nanoparticle dissolution, thereby contributing to enhanced durability.[9–11] In addition, organic modification improves both the activity and durability of core–shell catalysts and high-entropy alloys, which are more active than Pt nanoparticles.[7,10,13]

However, modifiers such as melamine do not exhibit intrinsic ORR catalytic activity; therefore, excessive dosing can poison the surface of Pt nanoparticles.[11] To maximise the enhancement effects of organic modification, the adsorption amount of the molecules should be optimised. This optimisation requires precise control of the interactions between organic molecules and Pt surfaces, and establishing theoretical guidelines for such interaction control remains an urgent task.

In prior works, two guidelines were established for the control: (1) the interaction energies correlate with the electron-donating ability of substituents on the triazine ring[17] and (2) the interaction is weaker for *N* in the triazine ring (N_{tri}) than for *N* in the amino group (N_{amino}) owing to the deeper energy position of the N_{tri} 2p orbital relative to the Fermi energy of Pt.[19] This study aims to provide further guidelines for molecular design based on quantum chemistry by systematically investigating the adsorption of melamine-like compounds onto Pt(111) using density functional theory (DFT).

The computational procedure is described in Supplementary Note 1 (SI). Briefly, the exchange–correlation functional employed was GGA-PBE.[27] Grimme's dispersion corrections were applied.[28,29] The Vienna *Ab initio* Simulation Package (VASP)[30–33] was used for the DFT calculations. Molecular orbital analyses were performed using the Gaussian16 programme.[34]

ORR activity was measured electrochemically using a rotating disk electrode, as described in ref. 11. Briefly, the ORR activity was first measured in the absence of modifiers. A modifier was then added to the electrolyte solution at a concentration of 1 μM, and the ORR activity was measured again without an incubation period. The ratio of the mass activities at 0.95 V (anodic scan) after and before the addition of a modifier is denoted as R_{ORR} and was used to evaluate its effect on ORR activity.

[a] *Research Institute of Electrochemical Energy (RIECEN), Department of Energy and Environment, National Institute of Advanced Industrial Science and Technology (AIST), 1–8–31 Midorigaoka, Ikeda, Osaka 563–8577, Japan. E-mail: tada.kohei.es@osaka-u.ac.jp*

[b] *Department of Materials Engineering Science, Graduate School of Engineering Science, The University of Osaka, Toyonaka, Osaka 560-8531, Japan*

[c] *Innovative Catalysis Science Division, Institute for Open and Transdisciplinary Research Initiatives (ICS-OTRI), The University of Osaka, Suita 565-0871, Osaka, Japan*

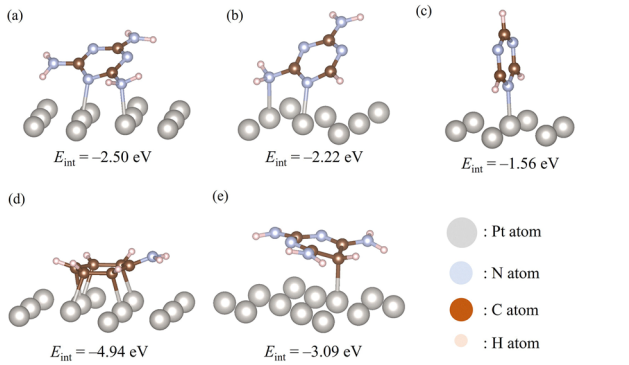

Fig. 1 Most stable adsorption structures of (a) melamine, (b) diamino-triazine, (c) triazine, (d) aniline, and (e) triamino-pyrimidine onto Pt(111).

Based on the energy landscapes obtained from the scans described in Supplementary Note 1 (SI), geometry optimisations were performed. The approach employed here successfully yielded the most stable adsorption structures of melamine and diamino-triazine (Fig. 1(a) and (b)), which are consistent with those reported previously.[17,19] The E_{int} values indicate that melamine interacts more strongly with Pt than diamino-triazine. This can be explained by the electron-donating ability of the substituents. The greater donating ability results in stronger Pt–N coordination bonds.[17] Therefore, melamine, which has more amino groups, undergoes larger interaction with Pt. This result is consistent with prior theoretical studies[17] and experimental findings.[6,11]

A previous study[23] reported the adsorption structures of melamine (triamino-triazine), diamino-triazine, and mono-amino-triazine on Pt(111). These molecules exhibit ORR activity enhancement effects.[6] This raises the question of how triazines without amino groups behave. The most stable structure of triazine/Pt(111) by DFT is shown in Fig. 1(c). Triazine is adsorbed perpendicular to the Pt(111) surface, whereas the planar adsorption structure is 0.7 eV less stable (see Fig. S3 in the SI). The adsorption structure of triazine on Pt(111) therefore differs markedly from that of benzene.[35,36] Compared with melamine/Pt(111), the E_{int} is approximately 1 eV weaker; thus, it is questionable whether triazine can remain stably adsorbed on the Pt surface under PEFC operating conditions.

Next, to investigate molecules lacking N_{tri} but containing N_{amino} atoms, the adsorption structure of aniline on Pt(111) was determined. As shown in Fig. 1(d), the most stable adsorption structure is planar, with bonding *via* multiple carbon atoms. In this adsorption state, the carbon atoms exhibit orbitals close to sp^3 hybridisation. This adsorption structure is similar to those of benzene and aniline derivatives.[35–37] The Pt–aniline interaction is 2.5 eV stronger than that for melamine. Such strong planar adsorption will result in over molecular coating of the Pt surface, thereby inhibiting the approach of reactant species O_2. Hence, the interaction between aniline and Pt will be too strong for effective use in organic modification.

Molecules without N_{tri} cannot exhibit surface-inclined adsorption on Pt(111) as observed for melamine. To investigate the lower limit of N_{tri} content, the adsorption of triamino-pyrimidine on Pt(111), which contains one fewer N_{tri} than melamine, was calculated. Despite the reduction of only one N_{tri}, the most stable adsorption structure of triamino-pyrimidine was planar (Fig. 1(e)). The adsorption mechanism is discussed later. The interaction energy was 0.6 eV larger than that for melamine and 2 eV smaller than that for aniline. Although triamino-pyrimidine may poison the Pt surface in a manner similar to aniline, its effect is expected to be less pronounced.

Molecules with strong adsorption, such as aniline, act as catalyst poisons, whereas molecules with weak adsorption, such as triazine, result in ineffective modification. If this assumption is correct, the ORR activity enhancement induced by molecular modifiers should exhibit an optimum region (or value) with respect to the strength of the molecule–surface interaction. To examine this hypothesis, the ORR activities of Pt nanoparticles modified with melamine, diamino-triazine, triazine, aniline, and triamino-pyrimidine were measured, for which the interaction energies with Pt(111) were evaluated in the present study. Fig. 2(a) shows a plot of the interaction energy E_{int} *versus* the ORR enhancement effect (R_{ORR}). The experimentally obtained linear sweep voltammograms used to estimate R_{ORR} are presented in the SI (Fig. S6). A volcano-shaped relationship is observed, indicating that melamine and diamino-triazine are located near the peak (optimal region). It should be noted that this volcano-shape is not caused by changes in the d-band centre of Pt. As described in prior studies,[18,20] melamine destabilises the intermediate OH by weakening the hydrogen-bond network. The change in the electronic state on the Pt surfaces is localised, therefore, the d-band centre, which is inherently delocalised, does not change upon melamine adsorption.[17–19] This is because the N–Pt bond is a coordinate bond, as confirmed by the differential charge distributions. As shown in Fig. 3, the changes in the electronic structure of Pt by molecular adsorptions investigated are localised. The results in Fig. 3 imply that the Pt–molecule interactions are governed by localised interactions such as coordination bonding.

A similar volcano-shaped trend is also observed in the plot of adsorption angle *versus* R_{ORR} (Fig. 2(b)), because the interaction energy correlates with the adsorption angle (see Fig. S7 in the SI). These results indicate that strong interactions associated with planar adsorption structures poison the Pt surface, whereas weak interactions associated with orthogonal

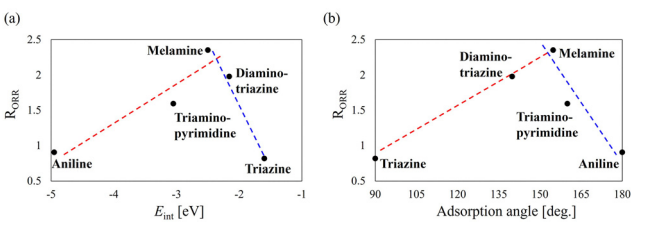

Fig. 2 (a) Volcano plot of molecule–surface interaction energy (E_{int}) and ratio of ORR activity before and after molecular modification (R_{ORR}). (b) Volcano plot of adsorption angle and R_{ORR}. Blue and red dotted lines indicate visual guides for trend interpretation.

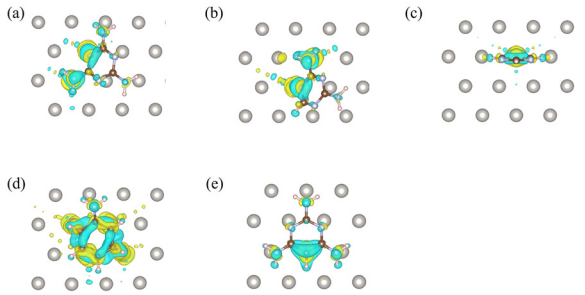

Fig. 3 Top views of charge difference distributions between before and after adsorptions for the most stable structures of melamine/Pt (a), diamino triazine/Pt (b), triazine/Pt (c), aniline/Pt (d), and triamino-pyrimidine/Pt (e). The threshold is 0.004 e^{-} $Bohr^{-3}$.

adsorption structures are ineffective. To further examine the hypothesis that the volcano-shaped distribution in Fig. 2 arises from adsorption strength and geometry, the key factors governing adsorption energy and structure are discussed below from the perspective of local electronic states associated with Pt–molecule bonds.

The weak interaction between triazine and Pt(111) arises because coordination through N_{tri} is weaker than that through N_{amino}. This difference between N_{tri} and N_{amino} was discussed in our previous work on melamine and explained using Frontier orbital theory.[19] Accordingly, the distribution and energy of occupied Frontier molecular orbitals will be critical, and these are summarised in Fig. S8–S13 (SI). Because the interactions between Pt and molecules are coordination bonds, the highest occupied molecular orbital (HOMO) will dominate the interactions (Fig. 4). We then summarise the HOMO in Fig. 5(a–e).

First, triazine and its derivatives—melamine (Fig. 5(a)), diamino-triazine (Fig. 5(b)), and triazine (Fig. 5(c))—are considered. Resonance stabilisation occurs between the p_z orbitals of N_{amino} and the π-conjugated system; thus, the p_z orbital of N_{amino} is not independent of the π-conjugation. As a result, the energy level of the N_{amino} p_z orbital is raised owing to electron cloud repulsion, and antibonding interactions between the p_z and π-orbitals of the triazine ring are evident in the HOMOs of melamine (Fig. 5(a)) and diamino-triazine (Fig. 5(b)). In contrast, the lone pair of N_{tri} is oriented perpendicular to the π-conjugated orbitals and remains independent of the π system. Consequently, the HOMO level of triazine is significantly deeper than those of the other molecules investigated (Fig. 5(a–e)). For melamine, the N_{tri} lone pair appears in the

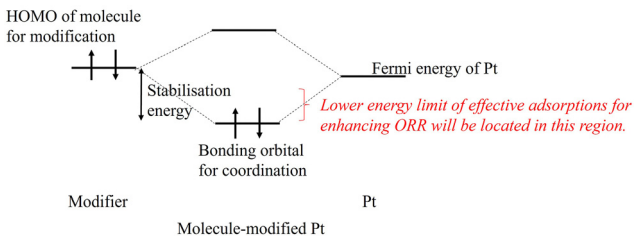

Fig. 4 Schematic view of coordination bonds between Pt and the modifier.

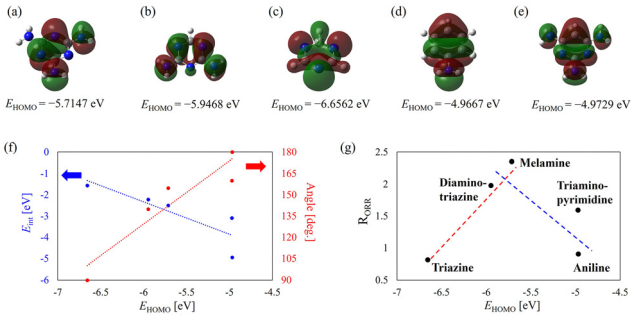

Fig. 5 HOMOs of (a) melamine, (b) diamino-triazine, (c) triazine, (d) aniline, and (e) triamino-pyrimidine. (f) HOMO energy levels (E_{HOMO}) *versus* molecule–Pt(111) interaction energy (E_{int}) and adsorption angle. (g) Volcano plot of R_{ORR} *versus* HOMO energy levels. Blue and red dotted lines indicate visual guides for trend interpretation.

HOMO−2, while for diamino-triazine, it appears in the HOMO−1 and HOMO−2. Previous work demonstrated that the deeper energy level of N_{tri} in melamine leads to a weaker interaction between N_{tri} and Pt than between N_{amino} and Pt[19]; the underlying rationale is shown in Fig. 4 and specific orbital energies are summarised in Fig. S13 (SI). Because the HOMO level of triazine is deeper than the HOMO−2 level of melamine (see Fig. 5(c) and Fig. S13), triazine exhibits only weak interaction with Pt(111). Furthermore, similar to a previous study,[19] we estimated the energy difference between the HOMO of the modifiers and the d-band centre of Pt(111) (see Supplementary Note 2 in the SI). The estimated values are 2.07 eV (melamine), 1.89 eV (diamino-triazine), and 1.24 eV (triazine). This order is consistent with the E_{int} values shown in Fig. 1. Moreover, analysis of the density of states (Fig. S15 in the SI) confirmed that the HOMO position of triazine is deeper than the HOMO−2 levels of both melamine and diamino-triazine. Consequently, the adsorption stabilisation in organic compounds containing a triazine ring can be tuned by adjusting the HOMO positions.

The strong adsorption of aniline can also be explained in terms of its Frontier orbitals. The HOMO energy of aniline is 0.8 eV higher than that of melamine (Fig. 5(a and d)); therefore, the stabilisation arising from coordination bonding is substantially greater than that for melamine. As shown by the HOMO distribution of aniline (Fig. 5(d)), two bonding π orbitals are present, one localised on C1, C2, and C6, and the other on C3, C4, and C5. In addition, the HOMO−1 of aniline (Fig. S11) contains bonding π orbitals on C2–C3 and C5–C6. The orbital energy of the HOMO−1 is close to that of the HOMO−2 in melamine and diamino-triazine (Fig. S13); thus, the HOMO−1 of aniline also contributes to its adsorption on Pt(111). Coordination involving the HOMO and HOMO−1 of aniline destabilises the benzene ring, as these orbitals contain bonding π-orbitals and the occupied electrons that are utilised in coordination. However, the stabilisation gained from Pt–C bond formation outweighs this destabilisation because of the high HOMO energy, leading to a change in carbon hybridisation from sp^2 to sp^3. Consequently, aniline adopts a planar adsorption structure.

The HOMO energy of triamino-pyrimidine is high, similar to that of aniline (Fig. 3(e)), leading to strong adsorption on Pt(111). However, the loss of electron resonance with the amino groups causes significant destabilisation of the triazine ring and Pt–N bonds, as previously discussed for melamine/Pt systems.[17,19] Furthermore, the π-electron density on the hetero-nitrogen atoms in the HOMO is low; therefore, these N atoms are ineffective for adsorption according to Frontier orbital theory. As shown in the HOMO distribution (Fig. 5(e)), relatively localised orbitals are instead found on the C–H bonds. Consequently, the C–H bonds contribute more to adsorption than the N atoms in triamino-pyrimidine, resulting in an adsorption structure involving a C–Pt bond (Fig. 1(e)). The adsorption of triamino-pyrimidine on Pt *via* a single carbon atom is further confirmed by the charge-density difference distribution shown in Fig. 3(e), where only the Pt atom bonded to carbon exhibits a change in electronic state. This behaviour contrasts with that of the aniline/Pt(111) system, in which electronic state changes extend across the entire benzene ring. Triamino-pyrimidine adopts an almost horizontal adsorption geometry but has only a single adsorption site. As a result, its adsorption angle will be sensitive to experimental conditions. In particular, the ORR measurements were conducted in the liquid phase, where solvent effects from water can influence molecular adsorption. Moreover, an applied electrode potential during ORR measurements can further affect adsorption behaviour. Consistent with these considerations, a clear difference in ORR activity is observed between triamino-pyrimidine and aniline.

Based on the results and discussion mentioned above, the E_{int} and adsorption angle will correlate with the HOMO energies, which can be confirmed from Fig. 5(f). Having already established the volcano-shaped correlations between E_{int} and R_{ORR}, and between the adsorption angle and R_{ORR}, we next examine the correlation between HOMO energy and R_{ORR} (Fig. 5(g)). A volcano-shaped trend is also observed for HOMO energy, although it is less pronounced than in the E_{int}–R_{ORR} plot. Notably, in the HOMO–R_{ORR} plot, the difference in enhancement effects between aniline and triamino-pyrimidine is not clearly distinguished. As discussed previously, this arises from the differing adsorption geometries of triamino-pyrimidine and aniline. Triamino-pyrimidine adsorbs *via* a single carbon atom, and its adsorption geometry will be sensitive to solvent and electrode potential. Note that we confirmed that the hybridisation peaks corresponding to the coordination bonds are located below $E - E_F = -4.5$ eV (Fig. S14); therefore, the bonds are not expected to break due to a downshift of the Fermi energy of Pt owing to the cathodic potential. However, the electrostatic interactions induced by the potential may lead to geometric changes. We also found that the d-band centre of the Pt atoms in the absence of adsorbed molecules remains the same (Table S1 in the SI). In addition, the HOMO levels of the molecules in the models with Pt (Fig. S14(a–c)) can be corrected using the energy difference relative to that of the gas phase (Table S2 in the SI). Therefore, orbital diagrams for the HOMOs can be constructed using the energy alignment relative to the constant d-band centre value (Fig. 6). The HOMO levels of the modifiers are slightly upshifted owing to distortions caused by the adsorption. Moreover, the energy differences between the HOMOs of the distorted modifiers and the main hybridisation peaks (ΔE) are correlated with the E_{int} values (Fig. 6). These results indicate that the interaction energy and adsorption structure of the investigated systems are primarily governed by the HOMOs of the molecules. Hence, analysing the HOMO of organic molecules is crucial for evaluating their effect on enhancing ORR activity.

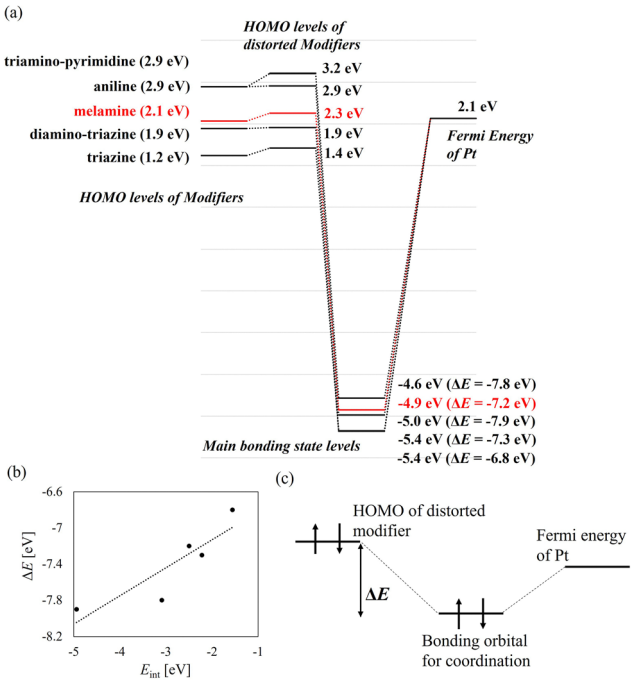

Fig. 6 (a) Orbital diagram of the HOMOs of the modifiers and the Fermi energy of Pt. The energies are aligned with the d-band centre of Pt (the details of the energy alignment are provided in Supplementary Note 2 in the SI). (b) Correlation between ΔE and E_{int} values. (c) Explanation of the ΔE value.

The adsorption of melamine analogues—melamine, diamino-triazine, triazine, aniline, and triamino-pyrimidine—onto Pt(111) was investigated using DFT. The adsorptions of melamine and diamino-triazine are weaker than that of aniline, and these molecules adopt tilted adsorption structures relative to the Pt(111). Consequently, melamine and diamino-triazine do not fully cover or poison the Pt surface as strongly horizontal adsorbing molecules like aniline do, resulting in less inhibition of the ORR. In contrast, the adsorption of triazine is markedly weaker than that of the other investigated molecules, indicating lower stability of the adsorption structure. Therefore, the ORR activity enhancement induced by molecular modifiers exhibits an optimum region (or value) with respect to the strength of the molecule–surface interaction. The adsorption structures and stabilisation of these molecules can be explained in terms of their occupied molecular orbitals. The HOMO is the dominant orbital, and a volcano-shaped correlation was observed between HOMO energy and ORR activity enhancement for the investigated molecules. Because numerous other factors influence the ORR, the

HOMO of coexisting organic molecules does not solely determine ORR activity. However, the HOMO energy of molecules can be readily estimated using standard quantum chemistry software; hence, we anticipate that the insights presented will accelerate the development of organic-modified catalysts.

Author contributions

K.T. conceived the study. K.T. and S.K. performed the theoretical calculations, and the results were analysed by K.T. and Yu.K. The theoretical section was validated by Ya.K. S.Y. prepared the molecularly modified Pt catalysts and conducted the experimental ORR measurements. The experimental results were validated by T.I. The results were visualised by K.T. and S.K. K.T. wrote the original draft with input from Yu.K., S.Y., M.A., and Y.C. All authors commented on the draft, and K.T. revised it. K.T. and T.I. secured the funding, and T.I. served as the project administrator and the supervisor.

Conflicts of interest

There are no conflicts to declare.

Data availability

The data supporting this article have been included as part of the supplementary information (SI). SI includes Computational procedures (Supplementary Note 1), Stable adsorption structures (Fig. S1, S2, S3, S4, and S5), Experimental LSV data (Fig. S6), Relationship between E_{int} and adsorption angle (Fig. S7), Molecular orbitals (Fig. S8, S9, S10, S11, and S12), Schematic orbital diagram for Pt adsorptions (Fig. S13), PDOS data for the most stable adsorption structures (Fig. S14), Energy alignment scheme (Supplementary Note 2), PDOS data for estimating the HOMO position relative to the d-band centre (Fig. S15), Values of d-band centre (Table S1), Comparison of HOMO levels (Table S2), and Specific coordinates of the most stable adsorption structures. Supplementary information is available. See DOI: https://doi.org/10.1039/d6cp00348f.

Acknowledgements

This study was partially supported by Project JPNP25002 commissioned by the New Energy and Industrial Technology Development Organization (NEDO). This study was conducted under the auspices of the Japan Society for the Promotion of Science (JSPS KAKENHI, grant no. JP25K08589). Part of the calculations were performed using the facilities of the Research Institute for Information Technology, Kyushu University. We would like to thank Editage (www.editage.jp) for English language editing.

Notes and references

1 D. A. Cullen, K. C. Neyerlin, R. K. Ahluwalia, R. Mukundan, K. L. More, R. L. Borup, A. Z. Weber, D. J. Myers and A. Kusoglu, *Nat. Energy*, 2021, **6**, 462, DOI: 10.1038/s41560-021-00775-z.
2 T. Ioroi, Z. Siroma, S. Yamazaki and K. Yasuda, *Adv. Energy Mater.*, 2019, **9**, 1801284, DOI: 10.1002/aenm.201801284.
3 K. Kodama, T. Nagai, A. Kuwaki, R. Jinnouchi and Y. Morimoto, *Nat. Nanotechnol.*, 2021, **16**, 140, DOI: 10.1038/s41565-020-00824-w.
4 S. Yamazaki, M. Asahi and T. Ioroi, *Electrochim. Acta*, 2019, **297**, 725, DOI: 10.1016/j.electacta.2018.11.165.
5 S. Yamazaki, M. Asahi, N. Taguchi and T. Ioroi, *J. Electroanal. Chem.*, 2019, **848**, 113321, DOI: 10.1016/j.jelechem.2019.113321.
6 M. Asahi, S. Yamazaki, N. Taguchi and T. Ioroi, *J. Electrochem. Soc.*, 2019, **166**, F498, DOI: 10.1149/2.0641908jes.
7 S. Yamazaki, M. Asahi, N. Taguchi, T. Ioroi, Y. Kishimoto, H. Daimon, M. Inaba, K. Koga, Y. Kurose and H. Inoue, *ACS Catal.*, 2020, **10**, 14567, DOI: 10.1021/acscatal.0c03124.
8 N. Wada, M. Nakamura and N. Hoshi, *Electrocatalysis*, 2020, **11**, 275, DOI: 10.1007/s12678-020-00584-0.
9 S. Yamazaki, M. Asahi, N. Taguchi and T. Ioroi, *J. Electroanal. Chem.*, 2022, **908**, 116103, DOI: 10.1016/j.jelechem.2022.116103.
10 H. Daimon, S. Yamazaki, M. Asahi, T. Ioroi and M. Inaba, *ACS Catal.*, 2022, **12**, 8976, DOI: 10.1021/acscatal.2c01942.
11 S. Yamazaki, M. Asahi, N. Taguchi and T. Ioroi, *Electrochim. Acta*, 2023, **472**, 143417, DOI: 10.1016/j.electacta.2023.143417.
12 N. Hoshi, M. Nakamura, R. Kubo and R. Suzuki, *Commun. Chem.*, 2024, **7**, 23, DOI: 10.1038/s42004-024-01113-6.
13 T. Kobayshi, Y. Chida, N. Todoroki and T. Wadayama, *ACS Catal.*, 2024, **14**, 11512, DOI: 10.1021/acscatal.4c02191.
14 S. Tanaka, H. Hattori, T. Koganezawa, T. Nakatani, R. Kumara, O. Sakata, K. Miyatake, N. Hoshi and M. Nakamura, *Int. J. Hydrogen Energy*, 2025, **172**, 151318, DOI: 10.1016/j.ijhydene.2025.151318.
15 B. Hammer and J. K. Nørskov, *Nature*, 1995, **376**, 238, DOI: 10.1038/376238a0.
16 A. Kulkarni, S. Siahrostami, A. Patel and J. K. Nørskov, *Chem. Rev.*, 2018, **118**, 2302, DOI: 10.1021/acs.chemrev.7b00488.
17 K. Tada, S. Yamazaki, M. Asahi and T. Ioroi, *Phys. Chem. Chem. Phys.*, 2023, **25**, 23047, DOI: 10.1039/D3CP01777J.
18 R. Jinnouchi and S. Minami, *J. Phys. Chem. Lett.*, 2025, **16**, 265, DOI: 10.1021/acs.jpclett.4c03437.
19 K. Tada, S. Yamazaki, M. Asahi and T. Ioroi, *Surf. Sci.*, 2025, **762**, 122817, DOI: 10.1016/j.susc.2025.122817.
20 Y. Katagiri, M. Nakamura and N. Hoshi, *J. Phys. Chem. C*, 2025, **129**, 13954, DOI: 10.1021/acs.jpcc.5c02481.
21 C. Clay, S. Haq and A. Hodgson, *Phys. Rev. Lett.*, 2004, **92**, 046102, DOI: 10.1103/PhysRevLett.92.046102.
22 V. Stamenkovic, B. S. Mun, K. J. J. Mayrhofer, P. N. Ross, N. M. Markovic, J. Rossmeisl, J. Greeley and J. K. Nørskov, *Angew. Chem., Int. Ed.*, 2006, **45**, 2897, DOI: 10.1002/anie.200504386.
23 I. E. L. Stephens, A. S. Bondarenko, F. J. Perez-Alonso, F. Calle-Vallejo, L. Bech, T. P. Johansson, A. K. Jepsen,

R. Frydendal, B. P. Knudsen, J. Rossmeisl and I. Chorkendorff, *J. Am. Chem. Soc.*, 2011, **133**, 5485, DOI: 10.1021/ja111690g.

24 K. Huang, T. Song, O. Morales-Collazo, H. Jia and J. F. Brennecke, *J. Electrochem. Soc.*, 2017, **164**, F1448, DOI: 10.1149/2.1071713jes.

25 R. Jinnouchi, K. Kodama and Y. Morimoto, *J. Electroanal. Chem.*, 2014, **716**, 31, DOI: 10.1016/j.jelechem.2013.09.031.

26 H. Shimada, Y. Ito, Y. Hanaoka, N. Hoshi and M. Nakamura, *Langmuir*, 2025, **41**, 19865, DOI: 10.1021/acs.langmuir.5c01815.

27 J. P. Perdew, K. Burke and M. Ernzerhof, *Phys. Rev. Lett.*, 1996, **77**, 3865, DOI: 10.1103/PhysRevLett.77.3865.

28 S. Grimme, J. Antony, S. Ehrlich and H. Krieg, *J. Chem. Phys.*, 2010, **132**, 154104, DOI: 10.1063/1.3382344.

29 S. Grimme, S. Ehrlich and L. Goerigk, *J. Comput. Chem.*, 2011, **32**, 1456, DOI: 10.1002/jcc.21759.

30 G. Kresse and J. Hafner, *Phys. Rev. B:Condens. Matter Mater. Phys.*, 1993, **47**, 558, DOI: 10.1103/PhysRevB.47.558.

31 G. Kresse and J. Hafner, *Phys. Rev. B:Condens. Matter Mater. Phys.*, 1994, **49**, 14251, DOI: 10.1103/PhysRevB.49.14251.

32 G. Kresse and J. Furthmüller, *Phys. Rev. B:Condens. Matter Mater. Phys.*, 1996, **54**, 11169, DOI: 10.1103/PhysRevB.54.11169.

33 G. Kresse and J. Furthmüller, *Comput. Mater. Sci.*, 1996, **6**, 15, DOI: 10.1016/0927-0256(96)00008-0.

34 M. J. Frisch, G. W. Trucks, H. B. Schlegel, G. E. Scuseria, M. A. Robb, J. R. Cheeseman, G. Scalmani, V. Barone, G. A. Petersson, H. Nakatsuji, X. Li, M. Caricato, A. V. Marenich, J. Bloino, B. G. Janesko, R. Gomperts, B. Mennucci, H. P. Hratchian, J. V. Ortiz, A. F. Izmaylov, J. L. Sonnenberg, D. Williams-Young, F. Ding, F. Lipparini, F. Egidi, J. Goings, B. Peng, A. Petrone, T. Henderson, D. Ranasinghe, V. G. Zakrzewski, J. Gao, N. Rega, G. Zheng, W. Liang, M. Hada, M. Ehara, K. Toyota, R. Fukuda, J. Hasegawa, M. Ishida, T. Nakajima, Y. Honda, O. Kitao, H. Nakai, T. Vreven, K. Throssell, J. A. Montgomery Jr., J. E. Peralta, F. Ogliaro, M. J. Bearpark, J. J. Heyd, E. N. Brothers, K. N. Kudin, V. N. Staroverov, T. A. Keith, R. Kobayashi, J. Normand, K. Raghavachari, A. P. Rendell, J. C. Burant, S. S. Iyengar, J. Tomasi, M. Cossi, J. M. Millam, M. Klene, C. Adamo, R. Cammi, J. W. Ochterski, R. L. Martin, K. Morokuma, O. Farkas, J. B. Foresman and D. J. Fox, *Gaussian16 RevA.03*, Gaussian, inc., Wallingford CT, 2016.

35 M. Saeys, M.-F. Reyniers, G. B. Marin and M. Neurock, *J. Phys. Chem. B*, 2002, **106**, 7489, DOI: 10.1021/jp0201231.

36 W. Liu, J. Carrasco, B. Santra, A. Michaelides, M. Scheffler and A. Tkatchenko, *Phys. Rev. B:Condens. Matter Mater. Phys.*, 2012, **86**, 245405, DOI: 10.1103/PhysRevB.86.245405.

37 T. Sheng, Y.-J. Qi, X. Lin, P. Hu, S.-G. Sun and W.-F. Lin, *Chem. Eng. J.*, 2016, **293**, 337, DOI: 10.1016/j.cej.2016.02.066.

